

FULL PAPER

Reflex-Based Open-Vocabulary Navigation without Prior Knowledge Using Omnidirectional Camera and Multiple Vision-Language Models

Kento Kawaharazuka^{a*}, Yoshiki Obinata^a, Naoaki Kanazawa^a, Naoto Tsukamoto^a,
Kei Okada^a, and Masayuki Inaba^a

^a*The Department of Mechano-Informatics, Graduate School of Information Science and Technology, The University of Tokyo, 7-3-1 Hongo, Bunkyo-ku, Tokyo, Japan.*

(Received 00 Month 201X; accepted 00 Month 201X)

Various robot navigation methods have been developed, but they are mainly based on Simultaneous Localization and Mapping (SLAM), reinforcement learning, etc., which require prior map construction or learning. In this study, we consider the simplest method that does not require any map construction or learning, and execute open-vocabulary navigation of robots without any prior knowledge to do this. We applied an omnidirectional camera and pre-trained vision-language models to the robot. The omnidirectional camera provides a uniform view of the surroundings, thus eliminating the need for complicated exploratory behaviors including trajectory generation. By applying multiple pre-trained vision-language models to this omnidirectional image and incorporating reflective behaviors, we show that navigation becomes simple and does not require any prior setup. Interesting properties and limitations of our method are discussed based on experiments with the mobile robot Fetch.

Keywords: Reflex-based Control, Omnidirectional Camera, Vision-Language Models

1. Introduction

Various navigation methods for robots have been developed so far. These methods often require prior learning and data collection, primarily through techniques such as Simultaneous Localization and Mapping (SLAM) and reinforcement learning. On the other hand, due to the high adaptability and responsiveness, behavior-based robot navigation methods have been developed for a long time. In this study, we consider performing open-vocabulary reflex-based navigation by combining these behavior-based navigation approaches with the advancements in current pre-trained vision-language models. We aim to achieve navigation in its simplest form without any prior learning, SLAM, or similar techniques, as illustrated in Fig. 1. For this purpose, we leverage omnidirectional cameras. By segmenting omnidirectional images and applying pre-trained vision-language models, we enable a reflex-based control that moves in the most appropriate direction according to instructions, eliminating the need for complex exploration actions including trajectory generation. Furthermore, we demonstrate that using multiple pre-trained vision-language models allows for more suitable navigation. Unlike previous research where maps or policies were generated in advance, this study intentionally avoids these steps and focuses on discussing how to achieve open-vocabulary navigation in the simplest manner possible. While each process itself is not new, combining them enables novel open-vocabulary reflex-based navigation.

This study is organized as follows. In Section 2, we discuss related navigation research based on map generation, reinforcement learning, and omnidirectional cameras. In Section 3, we describe the expansion of the omnidirectional image, the application of the multiple vision-language models, and the

*Corresponding author. Email: kawaharazuka@jsk.imi.i.u-tokyo.ac.jp

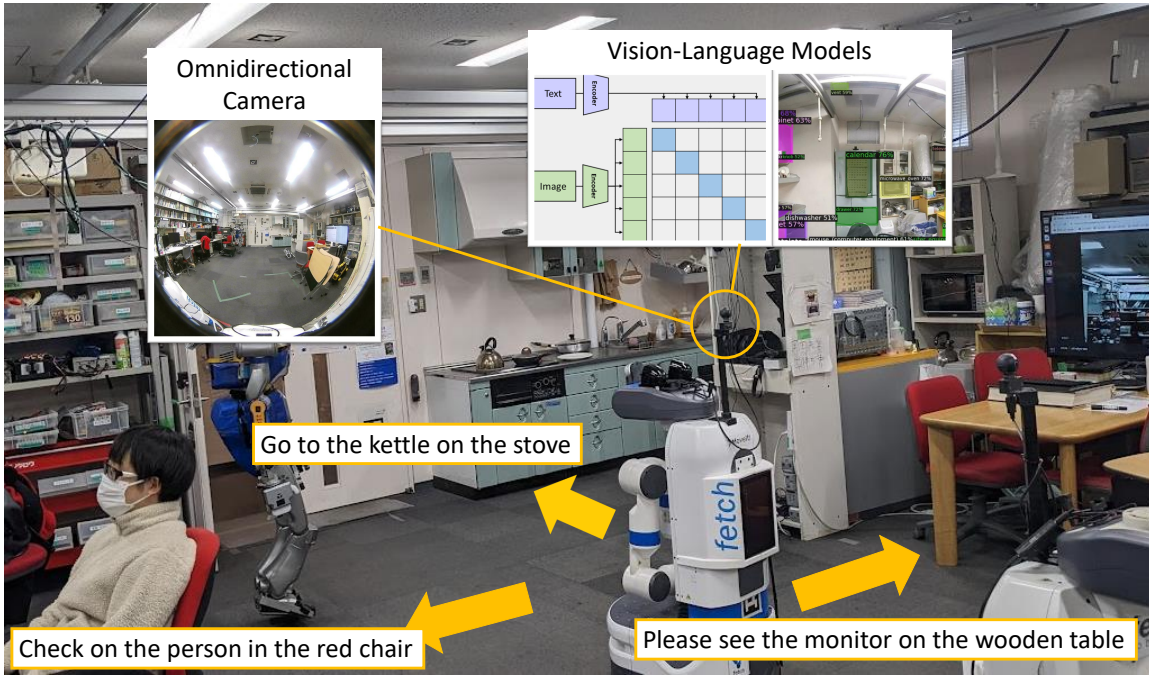


Figure 1. The concept of this study: simple reflex-based open-vocabulary navigation is enabled by splitting the expanded omnidirectional image and applying multiple pre-trained large-scale vision-language models.

reflex-based control based on linguistic instructions. In Section 4, we describe quantitative evaluation experiments and more practical advanced experiments. In Section 5, we discuss the experimental results and some limitations of this study, and conclude in Section 6.

2. Related Works

2.1 Navigation with Map Construction and Reinforcement Learning

Most of the robot navigation methods are based on Simultaneous Localization and Mapping (SLAM) [1, 2] or reinforcement learning [3]. In addition, the number of studies of open-vocabulary navigation has been increasing in recent years [4–9]. Embodied Question Answering (EmbodiedQA) [4] performs reinforcement learning-based path planning in which the robot searches for answers to questions in the simulation space. LM-NAV [5] combines Large Language Model (LLM), Vision-Language Model (VLM), and Visual Navigation Model (VNM) for path planning. However, EmbodiedQA [4] requires reinforcement learning in simulations, and LM-NAV [5] requires a large number of observations of the current environment for the construction of VNM. The same is true for methods such as CLIP-Fields [6], VLMaps [7], CLIP on Wheels [8], and ConceptFusion [9], and prior learning or data collection is indispensable. Therefore, there are few methods that allow real-world robots to start operating immediately in an environment with no prior knowledge.

2.2 Navigation with Omnidirectional Camera

The omnidirectional camera provides a uniform view of the surroundings and can be used for various tasks. Kobilarov et al. [10] has achieved human tracking using an omnidirectional camera and Laser Range Finder (LRF), and Marković et al. [11] has achieved dynamic object tracking. Rituerto et al. [12] has developed SLAM using an omnidirectional camera, Winters et al. [13] has developed navigation using a topological map with an omnidirectional camera, and Caron et al. [14] has realized visual servoing using an omnidirectional camera. On the other hand, these are not yet strongly linked to pretrained vision-language models. In this study, we apply the characteristic that the omnidirectional camera al-

lows the robot to understand the situation all around it, eliminating the need for complicated exploratory behaviors including trajectory generation, and enabling reflex-based navigation. In addition, we utilize multiple pre-trained vision-language models [15, 16] for open-vocabulary navigation.

2.3 Reflex-Based Navigation

In this study, “reflex” refers to the execution of low-level control such as direct joint angle and body velocity adjustments at a relatively fast frequency based on obtained sensory information. It also denotes a mechanism that directly associates sensory input with control command without requiring prior knowledge. Reflex-based robot navigation has been developed for a long time [17–22]. They have been mainly studied from the perspectives of fuzzy logic [20, 21], subsumption architecture [17, 18], morphological computation [22], and reinforcement learning [20]. On the other hand, their primary purposes are the movement to target positions represented as coordinates and collision avoidance, and open-vocabulary navigation is far from their scope.

3. Reflex-Based Open-Vocabulary Navigation Using Omnidirectional Camera and Pre-Trained Vision-Language Models

3.1 Omnidirectional Camera

In this study, we use Insta360 Air Camera (Arashi Vision Inc.), which is equipped with two fisheye lenses (front and rear). This camera has a combination of two fisheye lenses that can provide a 360-degree field of view. Here, the two fisheye images are expanded and combined together [23]. This process consists of four steps. First, fisheye lens intensity compensation is performed. In order to compensate for the optical phenomenon of vignetting, the pixel intensity is modified according to the distance from the center of the lens. Next, fisheye unwarping is performed. In order to produce a natural photographic image, each pixel is expanded by a geometric transformation in the order of unit sphere and square image. Then, the geometric misalignment between the two images is minimized from manual annotation in the overlapping regions. Finally, the two images are blended. The fisheye images before and after these steps are shown in Fig. 2. There are many unnecessary areas such as the ceiling and the robot’s head, at the top and bottom of the 2000×1000 expanded image. If this image is input to the vision-language models as it is, the information will become biased. Therefore, in practical use, we remove the lower and upper areas of the image, making it a 2000×500 image V as shown in the lower figure of Fig. 2.

3.2 Application of Pre-Trained Vision-Language Models

In this study, we use CLIP [15] and Detic [16] as pre-trained vision-language models. CLIP is a method to transform images and languages into vectors in the same embedding space, and Detic is a recognizer capable of detecting various classes of objects from images. Current VLMs are capable of four tasks: Generation Task, Understanding Task, Retrieval Task, and Grounding Task [24]. Among these, models like OFA [25] and BLIP2 [26], which are capable of Generation Task and Understanding Task, are relatively heavy in processing and not suitable for reflex-based control. On the other hand, Retrieval Task and Grounding Task have low computational cost and are suitable for this study. Models capable of Retrieval Task include CLIP [15] and ImageBind [27], while models capable of Grounding Task include Detic [16] and ViLD [28]. Among these models, we selected the representative models CLIP and Detic. Note that, for Detic, we use the object classes in LVIS [29] as objects to be detected.

First, the image obtained by Section 3.1 is split into N_{split} pieces. Here, there can be overlaps between the pieces. Next, CLIP and Detic are applied to the obtained split images V_i ($1 \leq i \leq N_{split}$). Let v_i^{clip} be a vector obtained by applying CLIP to V_i . From Detic, labels and bounding boxes of various objects are obtained. The detected labels are sorted in descending order by the size of the bounding box, and are separated by commas to form a sentence (e.g. “table, monitor, monitor, monitor, apple, knife”). This

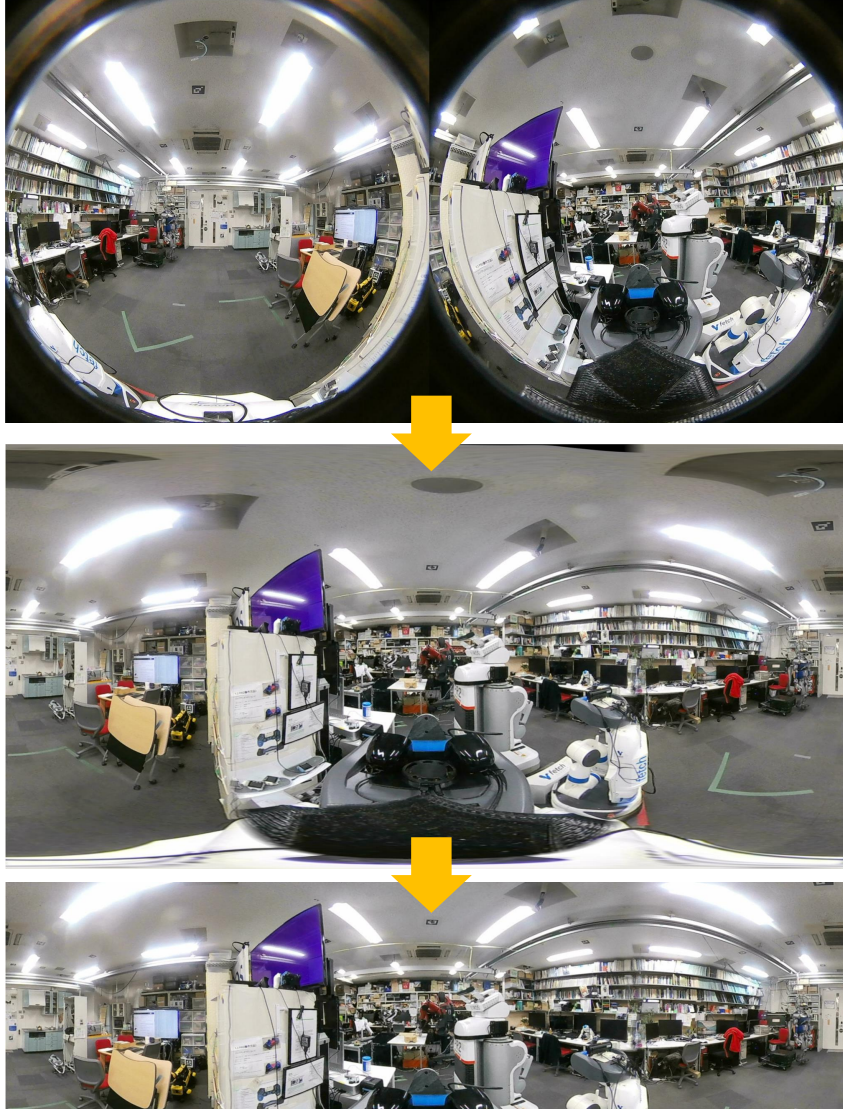


Figure 2. Dual-fisheye stitching for the expanded 360-degree omnidirectional image. The upper figure shows the fisheye images before processing, the middle figure shows the expanded image, and the lower figure shows the input image to vision-language models with unnecessary parts removed from the expanded image.

sentence is transformed into a vector v_i^{detic} by Sentence-BERT [30]. In practice, Detic is applied not to the split image V_i but to the expanded image V from the viewpoint of computation time, and the obtained result is split.

When the robot receives a linguistic instruction Q , it is transformed into a vector q^{clip} by CLIP and into a vector q^{detic} by Sentence-BERT. Assuming that the obtained vectors are all normalized, we obtain the following cosine similarity s and the transformed similarity a ,

$$s_i^{clip} = v_i^{clip} \cdot q^{clip} \quad (1)$$

$$a_i^{clip} = 0.1 + 0.9 \frac{s_i^{clip} - s_{min}^{clip}}{s_{max}^{clip} - s_{min}^{clip}} \quad (2)$$

$$s_i^{detic} = v_i^{detic} \cdot q^{detic} \quad (3)$$

$$a_i^{detic} = 0.1 + 0.9 \frac{s_i^{detic} - s_{min}^{detic}}{s_{max}^{detic} - s_{min}^{detic}} \quad (4)$$

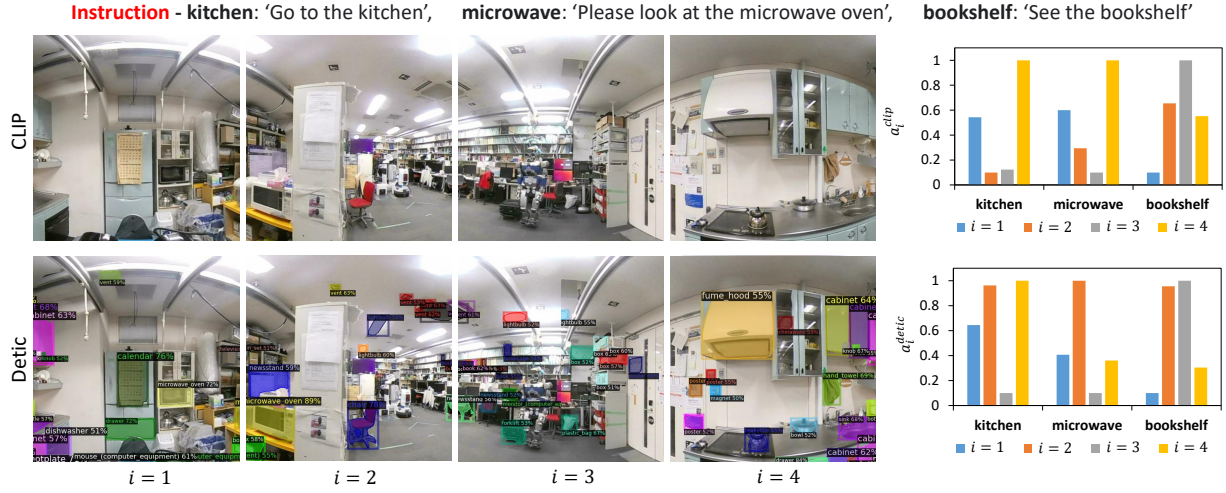


Figure 3. The preliminary experiments of using large-scale vision-language models for open-vocabulary navigation. The left figure shows the split image and the recognition result, and the right graph shows the average of the transformed similarity a for 10 repetitions of each instruction for CLIP and Detic: **kitchen** - “Go to the kitchen”, **microwave** - “Please look at the microwave oven”, **bookshelf** - “See the bookshelf”.

where $s_i^{\{clip,detic\}}$ denotes the minimum and maximum values of $s_i^{\{clip,detic\}}$ ($1 \leq i \leq N_{split}$). The minimum value of a is converted to 0.1 and the maximum value of a is converted to 1.0 in order to measure s_i^{clip} and s_i^{detic} on the same scale. Note that the minimum value is set to 0.1 instead of 0 because of the way it is used in Section 3.3.

As an example, the result for $N_{split} = 4$ is shown in Fig. 3. The following three instructions are given: **kitchen** - “Go to the kitchen”, **microwave** - “Please look at the microwave oven”, **bookshelf** - “See the bookshelf”. The right figure of Fig. 3 shows the average of a_i for 10 repetitions of each instruction when $i = \{1, 2, 3, 4\}$. First, in the case of **kitchen**, the images of $i = \{1, 4\}$ match the instruction. $a_{\{1,4\}}$ are high for CLIP as intended because it judges the similarity between the instruction and the image by looking at the image as a whole. On the other hand, Detic recognizes each object in the image separately. Therefore, Detic recognized the microwave oven, an object that is usually located in the kitchen, making a_2 as high as a_4 . Next, in the case of **microwave**, the microwave oven is actually in the image when $i = \{1, 2\}$. a_2 is high in Detic as intended because it recognizes individual objects. Note that a_1 is not so high because the bounding box of the microwave oven is small. On the other hand, CLIP sees the image as a whole and it misses individual objects, making a_2 low. Since the microwave oven is usually located in the kitchen, we can see that a_i in CLIP shows similar distributions in the cases of **microwave** and **kitchen**. Finally, in the case of **bookshelf**, the bookshelf is actually in the image when $i = \{2, 3\}$, and we can see that $a_{\{2,3\}}$ are high as intended for both models. Thus, depending on the vision-language model used, there are instructions that are good or bad at being recognized.

3.3 Mapping from Linguistic Instruction to Motion

We map $a_i^{\{clip,detic\}}$ obtained in Section 3.2 to the actual robot motion (Fig. 4). First, we calculate the following evaluation value e_i in order to resolve the problem that a_i^{clip} and a_i^{detic} each have its own strengths and weaknesses as described in Section 3.2.

$$e_i = a_i^{clip} a_i^{detic} \quad (5)$$

The minimum value of a_i is set to 0.1 as described in Section 3.2 to ensure that e_i does not become 0 even when either s_i^{clip} or s_i^{detic} is very small. By using such metrics, we accommodate scenarios where one of $s_i^{\{clip,detic\}}$ is small while the other is large. Next, we retrieve $N_{extract}$ number of e_i in descending order. Here, let \mathbf{b}_i be the unit direction vector toward which the center point of the image V_i faces, and let i_j be i of the j -th largest e_i ($1 \leq j \leq N_{extract}$). The direction vector \mathbf{b} that the robot should move toward

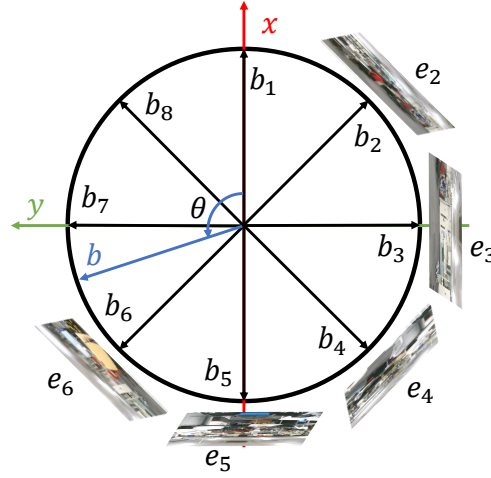


Figure 4. The configuration when mapping linguistic instructions to robot wheeled-base motion.

is calculated as follows.

$$\mathbf{b} = \sum_j (N_{extract} + 1 - j) \mathbf{b}_{ij} / \sum_j (N_{extract} + 1 - j) \quad (6)$$

This calculation is adopted to make a proper judgement based on the totality of the surrounding circumstances and to avoid the problem of falling into a local minima by making the robot move in the direction with the largest e_i . We map this \mathbf{b} to the robot motion. For an omnidirectional wheeled robot with omni wheels or mecamum wheels, it is sufficient to simply generate a translation speed in the direction of \mathbf{b} . On the other hand, for a two-wheeled robot, the mapping is as follows,

$$a_{linear} = 1.0 \quad \text{if } |\theta| < C_{thre} \quad (7)$$

$$a_{rotate} = k\theta \quad (8)$$

where $a_{\{linear, rotate\}}$ is the velocity of the robot in the translational and rotational direction ($\{\text{m/s, rad/s}\}$), θ is the angle between $(1 \ 0)^T$ and \mathbf{b} and is expressed from $-\pi$ to π , k is a proportionality constant, and C_{thre} is a threshold value. Note that the rotational directions of i and θ are different because the coordinate systems of the robot and the image are different.

3.4 Other Settings

In this study, we conduct experiments using the mobile robot Fetch. Since the robot is equipped with LRF, it can be constrained not to move in the direction of obstacles. Of course, it is possible to provide the robot with a bumper and a contact sensor, and to construct another reflective behavior for obstacle avoidance. By incorporating obstacle avoidance, the robot can stop appropriately without going too far in the target direction.

4. Experiments

In this study, we first demonstrate the performance of our method quantitatively in a small area surrounded on all sides. Then, we show a series of navigation experiments using our method in a larger space. In this study, we set $N_{split} = 8$, $C_{extract} = 2$, $C_{thre} = 0.6$ [rad], and $k = 0.5$, and the control of Section 3.3 is operated at 10 Hz. With $N_{split} = 8$, inference is performed at a maximum of 12 Hz for CLIP and 5 Hz for Detic on a machine equipped with an i7-6850K CPU and an Nvidia GeForce RTX 3090 GPU. While inference time for CLIP increases proportionally to N_{split} , inference time for Detic remains

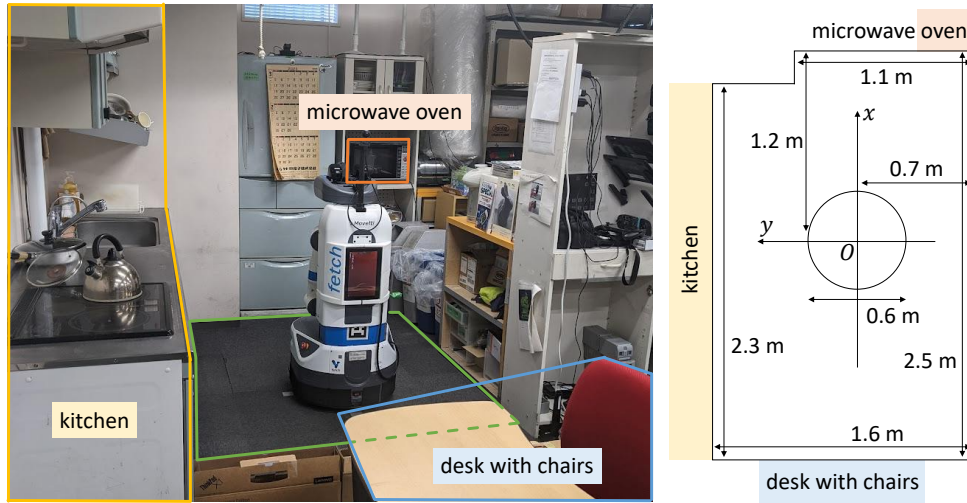


Figure 5. The environmental setup of the basic experiment. The mobile robot Fetch is placed in a small area surrounded by the kitchen, microwave oven, and desk with chairs.

independent of N_{split} as it is directly applied to the expanded image V .

4.1 Basic Experiment

The environmental setup for the basic experiment is shown in Fig. 5. An area is surrounded by shelves and walls on all four sides and is about 2.5×1.6 m in size. The footprint size of Fetch is about 0.6×0.6 m. In this experiment, we prepared three instructions: **kitchen** - “Go to the kitchen”, **microwave** - “Please look at the microwave oven”, and **desk** - “See the desk with chairs”. The kitchen, microwave oven, and desk with chairs are arranged as in Fig. 5. In this experiment, we compare three methods: the proposed method **ALL**, **CLIP** using only CLIP with $e_i = a_i^{clip}$, and **Detic** using only Detic with $e_i = a_i^{detic}$.

The results of five navigation experiments for each instruction using each of the three methods are shown in Fig. 6. The left figures show the trajectories of Fetch for each of the five navigation experiments. Note that Fetch is stopped when it touches the walls/shelves, or once 30 seconds have passed since the start of the experiment. Ideally, the robot should move toward “target” in Fig. 6, which is the center of the position indicated by the instruction, with “origin” as the initial position. However, in some cases, the error does not need to be zero because “kitchen” or “desk” can refer to a large area, but the error should be as small as possible. The right figure of Fig. 6 shows the average and variance of the error between the robot’s final position and the target position.

For **kitchen**, we can see that the robot moves correctly toward the kitchen when using the methods of **CLIP** and **ALL**. On the other hand, for **Detic**, the robot meanders and does not move in the expected direction. The final position error of **Detic** is larger than those of **CLIP** and **ALL**. Although the error of **CLIP** is slightly smaller than that of **ALL**, the performance is considered to be almost the same because of the wider area of the kitchen as mentioned above. For **microwave**, we can see that the robot moves correctly toward the microwave oven in the case of **ALL**. In the case of **Detic**, the robot moves toward the microwave oven to some extent, but its performance is not as good as that of **ALL** due to meandering. On the other hand, in the case of **CLIP**, the robot moves toward the kitchen and its performance is significantly worse. For **desk**, the performance is high in the order of **ALL**, **CLIP**, and **Detic**. It can be seen that the performance of **ALL** is the best throughout all the experiments.

4.2 Advanced Experiment

We conducted a series of navigation experiments in a larger space. By accepting continuous instructions in a wide space, it demonstrates the possibility of more practical navigation. The instructions were changed to the following: (1) “Look at the large TV display on the wooden table”, (2) “Look at the

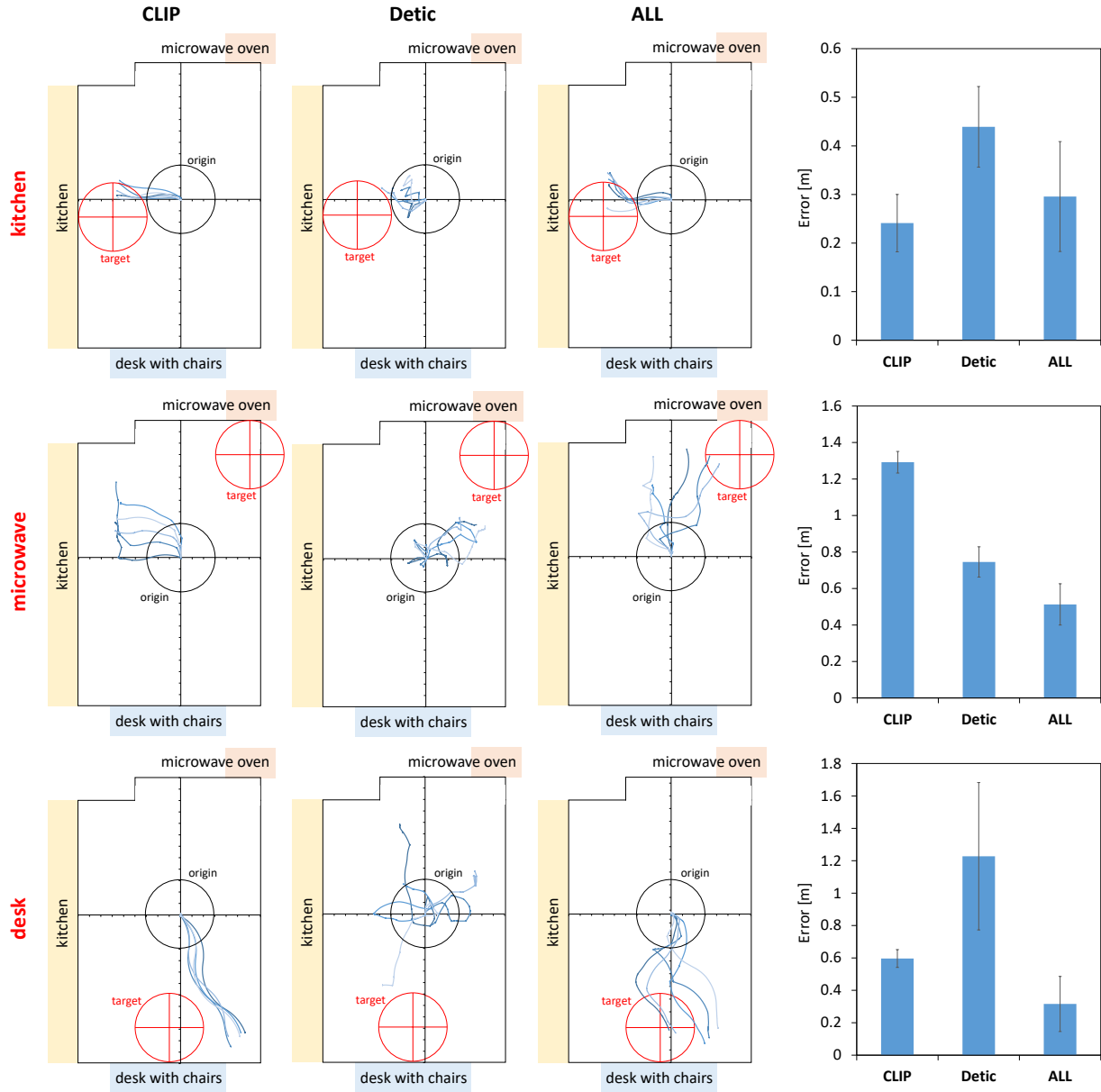


Figure 6. The trajectories of the mobile robot Fetch and the error between the robot's final and target positions in the basic experiment. We prepared three instructions: **kitchen** - "Go to the kitchen", **microwave** - "Please look at the microwave oven", and **desk** - "See the desk with chairs", and compared the proposed method **ALL** with **CLIP** and **Detic**.

multiple small PC monitors on the white desk near the bookshelf", (3) "Check the microwave oven". In this experiment, we use the proposed method **ALL**. The experimental environment and the trajectory of the robot are shown in Fig. 7. Here, the initial position "origin" of the robot and the center of the target position "target" are shown. However, as described in Section 4.1, the target position has some width, so "target" refers to only a rough position. The picture seen from "view-1" and "view-2" shown in Fig. 7, and the omnidirectional image of the camera are shown in Fig. 8. Note that ①–⑤ in Fig. 7 correspond to those in Fig. 8. Both (1) and (2) deal with the same class of objects such as the display and monitor, but by adding information such as wooden table, bookshelf, white desk, etc., they are correctly distinguished and intended navigation is possible at ② and ③. As for (3), the microwave oven is not visible at ③, but the robot is heading toward the kitchen at ④ where the microwave oven is usually located. Then the robot actually finds the microwave in the kitchen and stops in front of it at ⑤.

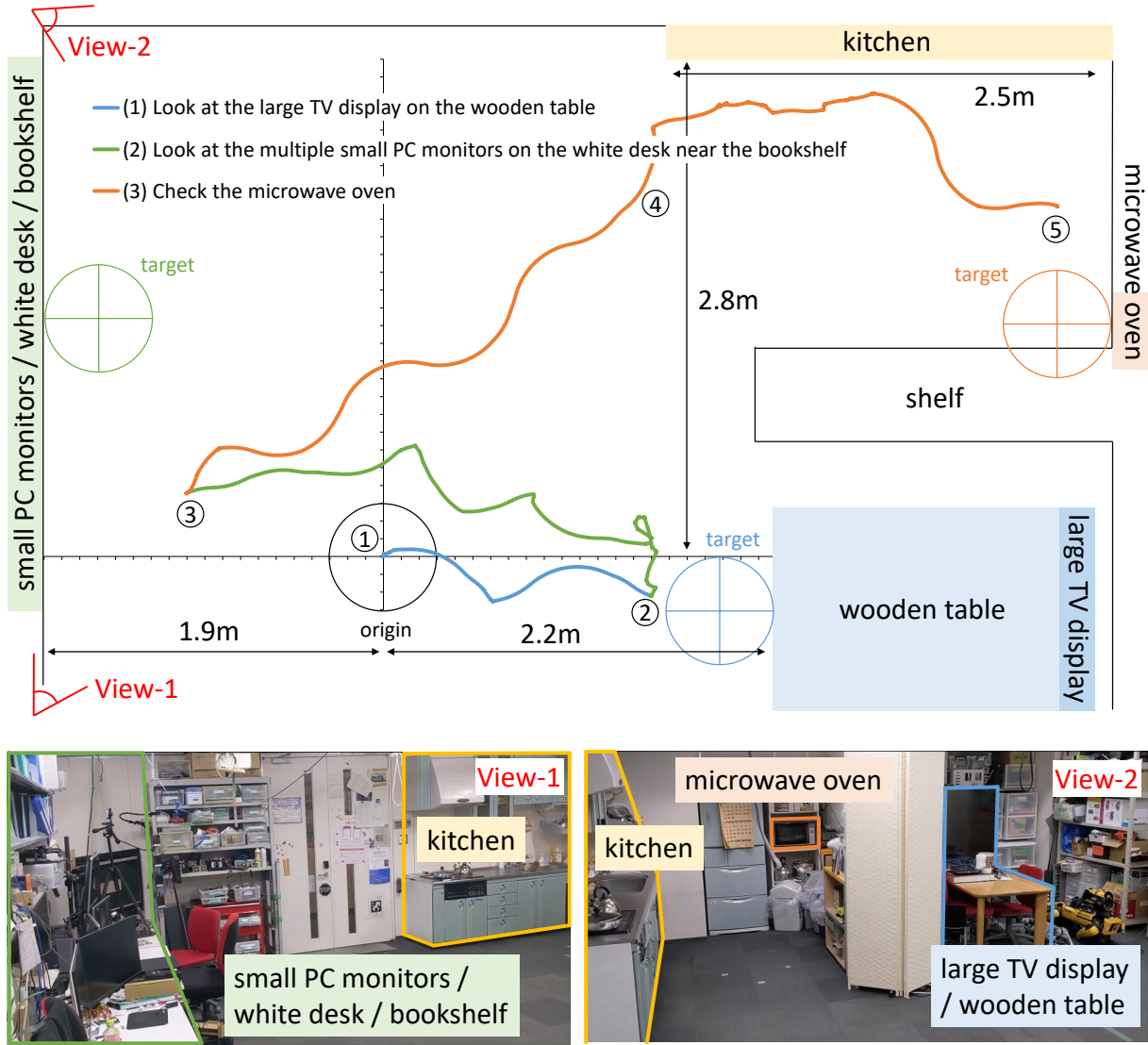


Figure 7. The trajectory of the mobile robot Fetch in the advanced navigation experiment.

5. Discussion

The results obtained are summarized below. First, the basic experiment shows that the robot can move to the appropriate position from linguistic instructions by splitting the expanded omnidirectional image, applying multiple pre-trained vision-language models, and controlling the wheels reflexively. **ALL**, which combines CLIP and Detic outputs, enables navigation with higher accuracy compared to either **CLIP** or **Detic**. As can be seen from the preliminary experiment in Section 3.2, CLIP alone can extract only global features of the image, while Detic alone can extract only local features of the image. The combination of these two models enables stable navigation. In addition, the robot moved without hesitation in the case of **CLIP**, while it has shown meandering movements in the case of **Detic**. This may be because the recognition results of Detic differ greatly from step to step. Next, the advanced experiment shows that navigation is possible even when the linguistic instructions are changed continuously. By adding various modifications to the linguistic instructions, it is possible to distinguish between similar objects and move in the appropriate direction. Also, we found that even when the robot is instructed to move toward an object that is not directly visible, it first moves in the direction in which the object is generally expected to exist, finds the indicated object, and then moves toward it. This is an interesting feature of the proposed system.

Limitations and future prospects of this study are described. First, several parameters in our method

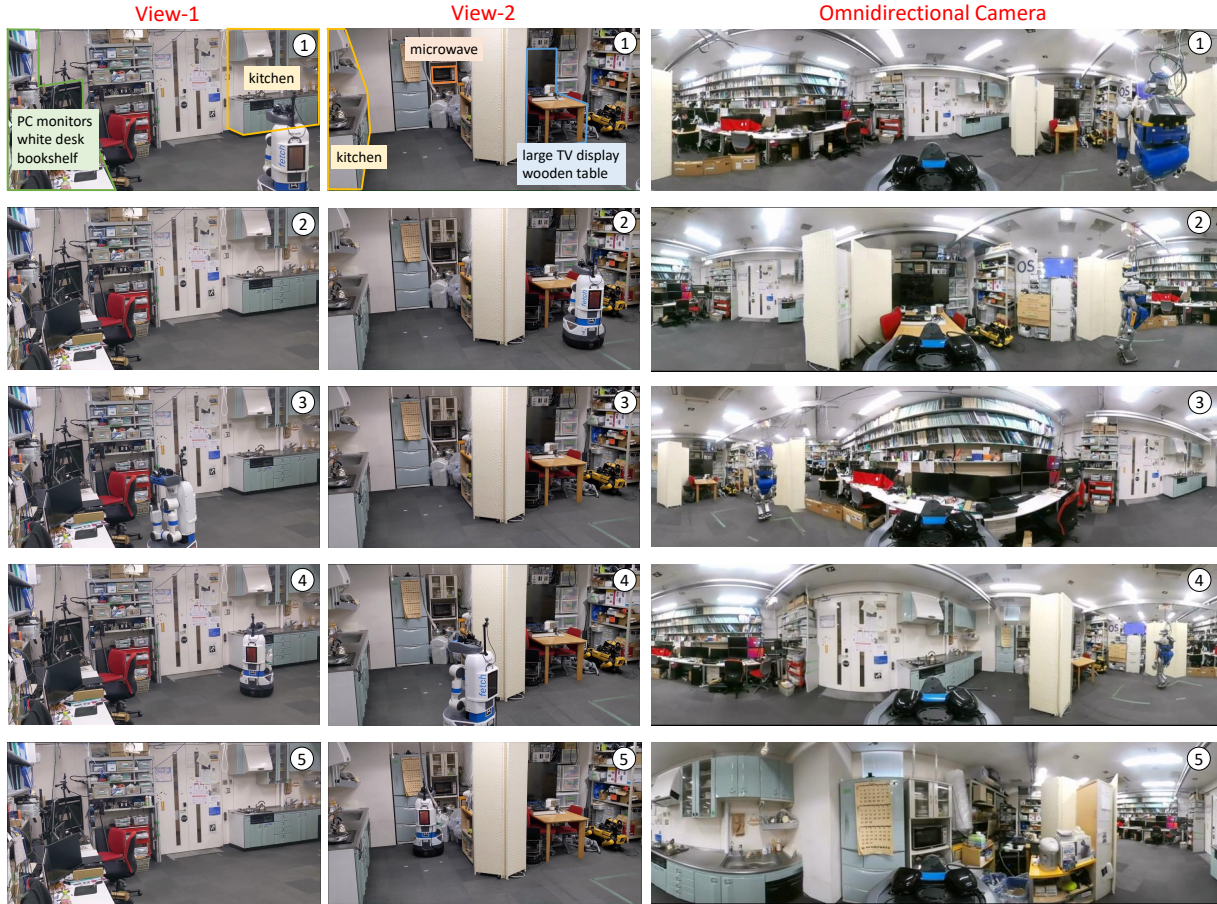


Figure 8. The advanced navigation experiment. The instruction is continuously changed in the following order: (1) “Look at the large TV display on the wooden table”, (2) “Look at the multiple small PC monitors on the white desk near the bookshelf”, and (3) “Check the microwave oven”.

must be manually tuned. In particular, the number of segmentations of the omnidirectional image is important, since increasing the number of segmentations increases the inference time while increasing the accuracy of the target direction, which is a trade-off. On the other hand, once the desired frequency for control is determined, it is only necessary to set the number of segmentations to fit that frequency, eliminating the need for prior experimentation. The degree of overlap of the split images is also important, and appropriate settings are necessary. Second, there is a limit to the types of instructions that can be recognized by the vision-language models. When there are multiple objects or environments that match the instruction, the model cannot navigate the robot well without appropriate modifications. In the case of Section 4.2, we observed that the robot would get lost and constantly rotate unless the instruction was modified by words such as “wooden table” or “bookshelf”. There is also a problem that the robot does not recognize negations well. The accuracy also varies depending on the size of the target object. These problems are currently open questions for general vision-language models, and we believe that more advanced navigation will become possible in the future with the development of these models. Third, navigation in more complex spaces is currently difficult for our method. There is no problem if the shape of the navigation area is convex, but it may be difficult to perform proper navigation if the shape is concave. In such cases, a possible solution is to guide the robot to the desired position by changing the instructions for intermediate landmarks. Also, we might be able to solve this problem if we can extract two types of information from language instructions: the direction to head towards and the direction to avoid. In the future, we would like to make more advanced reflex-based motion generation possible by adding exploratory behaviors to avoid obstacles and repetitive actions.

This study is the first example to demonstrate the compatibility of the omnidirectional camera and the vision-language models for reflex-based open-vocabulary navigation by using an actual mobile robot. The idea itself is simple, but by using multiple vision-language models in a split omnidirectional camera

image, it is possible to determine features of the surroundings both globally and locally, and to perform advanced navigation. We believe that this idea has potential applications not only for service robots in daily life, but also for complex and dangerous disaster sites.

6. Conclusion

In this study, we have described a reflex-based open-vocabulary navigation system using an omnidirectional camera and multiple pre-trained vision-language models. It does not require any prior knowledge, including map construction and learning. By using an omnidirectional camera, the robot can obtain information about its surroundings as a whole, and by splitting the image and applying pre-trained vision-language models to each image, the robot can determine which direction is most consistent with the current linguistic instructions. By mapping this direction to the robot's movements, we show that open-vocabulary navigation can be constructed in a simple reflex-based form. Moreover, by using multiple types of vision-language models, the robot can respond to a wider variety of linguistic instructions. We expect various applications of this idea in the future. On the other hand, there are cases where the system does not work well depending on the structure of the room or the objects to be recognized, and we would like to consider a more adaptive robot system that can respond to such situations without the need for prior knowledge.

References

- [1] M. R. U. Saputra, A. Markham, and N. Trigoni. Visual SLAM and structure from motion in dynamic environments: A survey. *ACM Computing Surveys*, Vol. 51, No. 2, pp. 1–36, 2018.
- [2] G. Grisetti, R. Kümmerle, C. Stachniss, and W. Burgard. A Tutorial on Graph-Based SLAM. *IEEE Intelligent Transportation Systems Magazine*, Vol. 2, No. 4, pp. 31–43, 2010.
- [3] K. Zhu and T. Zhang. Deep reinforcement learning based mobile robot navigation: A review. *Tsinghua Science and Technology*, Vol. 26, No. 5, pp. 674–691, 2021.
- [4] A. Das, S. Datta, G. Gkioxari, S. Lee, D. Parikh, and D. Batra. Embodied Question Answering. In *Proceedings of the 2018 IEEE/CVF International Conference on Computer Vision and Pattern Recognition*, 2018.
- [5] D. Shah, B. Osinski, B. Ichter, and S. Levine. Robotic Navigation with Large Pre-Trained Models of Language, Vision, and Action. In *Proceedings of the 2022 Conference on Robot Learning*, 2022.
- [6] N. M. M. Shafiullah, C. Paxton, L. Pinto, S. Chintala, and A. Szlam. CLIP-Fields: Weakly Supervised Semantic Fields for Robotic Memory. In *Proceedings of the 2020 Robotics: Science and Systems*, pp. 1–11, 2023.
- [7] C. Huang, O. Mees, A. Zeng, and W. Burgard. Visual Language Maps for Robot Navigation. In *Proceedings of the 2023 IEEE International Conference on Robotics and Automation*, pp. 10608–10615, 2023.
- [8] S. Y. Gadre, M. Wortsman, G. Ilharco, L. Schmidt, and S. Song. Cows on pasture: Baselines and benchmarks for language-driven zero-shot object navigation. In *Proceedings of the 2023 IEEE/CVF International Conference on Computer Vision and Pattern Recognition*, pp. 23171–23181, 2023.
- [9] K. M. Jatavallabhula, A. Kuwajerwala, Q. Gu, M. Omama, T. Chen, S. Li, G. Iyer, S. Saryazdi, N. Keetha, A. Tewari, J. B. Tenenbaum, C. M. Melo, M. Krishna, L. Paull, F. Shkurti, and A. Torralba. ConceptFusion: Open-set Multimodal 3D Mapping. *Proceedings of the 2020 Robotics: Science and Systems*, 2023.
- [10] M. Kobilarov, G. Sukhatme, J. Hyams, and P. Batavia. People tracking and following with mobile robot using an omnidirectional camera and a laser. In *Proceedings of the 2006 IEEE International Conference on Robotics and Automation*, pp. 557–562, 2006.
- [11] I. Marković, F. Chaumette, and I. Petrović. Moving object detection, tracking and following using an omnidirectional camera on a mobile robot. In *Proceedings of the 2014 IEEE International Conference on Robotics and Automation*, pp. 5630–5635, 2014.
- [12] A. Rituerto, L. Puig, and J. J. Guerrero. Visual SLAM with an Omnidirectional Camera. In *Proceedings of the 20th International Conference on Pattern Recognition*, pp. 348–351, 2010.
- [13] N. Winters, J. Gaspar, G. Lacey, and J. Santos-Victor. Omni-directional vision for robot navigation. In *Proceedings of the IEEE Workshop on Omnidirectional Vision*, pp. 21–28, 2000.

- [14] G. Caron, E. Marchand, and E. M. Mouaddib. Photometric visual servoing for omnidirectional cameras. *Autonomous Robots*, Vol. 35, No. 2, pp. 177–193, 2013.
- [15] A. Radford, J. W. Kim, C. Hallacy, A. Ramesh, G. Goh, S. Agarwal, G. Sastry, A. Askell, P. Mishkin, J. Clark, G. Krueger, and I. Sutskever. Learning Transferable Visual Models From Natural Language Supervision. In *Proceedings of the 38th International Conference on Machine Learning*, pp. 8748–8763, 2021.
- [16] X. Zhou, R. Girdhar, A. Joulin, P. Krähenbühl, and I. Misra. Detecting Twenty-thousand Classes using Image-level Supervision. In *Proceedings of the 2022 European Conference on Computer Vision*, 2022.
- [17] R. Brooks. A robust layered control system for a mobile robot. *IEEE Journal on Robotics and Automation*, Vol. 2, No. 1, pp. 14–23, 1986.
- [18] J. K. Rosenblatt and D. W. Payton. A fine-grained alternative to the subsumption architecture for mobile robot control. In *Proceedings of the 1989 International Joint Conference on Neural Networks*, pp. 317–323, 1989.
- [19] A. P. Duchon and W. H. Warren. Robot navigation from a Gibsonian viewpoint. In *Proceedings of the IEEE International Conference on Systems, Man and Cybernetics*, Vol. 3, pp. 2272–2277, 1994.
- [20] A. Dubrawski and J. L. Crowley. Learning locomotion reflexes: A self-supervised neural system for a mobile robot. *Robotics and Autonomous Systems*, Vol. 12, No. 3, pp. 133–142, 1994.
- [21] R. Chatterjee and F. Matsuno. Use of single side reflex for autonomous navigation of mobile robots in unknown environments. *Robotics and Autonomous Systems*, Vol. 35, No. 2, pp. 77–96, 2001.
- [22] F. Boyer, V. Lebastard, C. Chevallereau, and N. Servagent. Underwater Reflex Navigation in Confined Environment Based on Electric Sense. *IEEE Transactions on Robotics*, Vol. 29, No. 4, pp. 945–956, 2013.
- [23] T. Ho and M. Budagavi. Dual-fisheye lens stitching for 360-degree imaging. In *Proceedings of the 2017 IEEE International Conference on Acoustics, Speech and Signal Processing*, pp. 2172–2176, 2017.
- [24] F. Li, H. Zhang, Y. Zhang, S. Liu, J. Guo, L. M. Ni, P. Zhang, and L. Zhang. Vision-Language Intelligence: Tasks, Representation Learning, and Large Models. arXiv preprint arXiv:2203.01922, 2022.
- [25] P. Wang, A. Yang, R. Men, J. Lin, S. Bai, Z. Li, J. Ma, C. Zhou, J. Zhou, and H. Yang. OFA: Unifying Architectures, Tasks, and Modalities Through a Simple Sequence-to-Sequence Learning Framework. In *Proceedings of the 39th International Conference on Machine Learning*, pp. 23318–23340, 2022.
- [26] J. Li, D. Li, S. Savarese, and S. Hoi. BLIP-2: Bootstrapping Language-Image Pre-training with Frozen Image Encoders and Large Language Models. In *Proceedings of the 40th International Conference on Machine Learning*, pp. 19730–19742, 2023.
- [27] R. Girdhar, A. El-Nouby, Z. Liu, M. Singh, K. V. Alwala, A. Joulin, and I. Misra. ImageBind: One Embedding Space To Bind Them All. In *Proceedings of the 2023 IEEE/CVF International Conference on Computer Vision and Pattern Recognition*, 2023.
- [28] X. Gu, T. Lin, W. Kuo, and Y. Cui. Open-vocabulary Object Detection via Vision and Language Knowledge Distillation. In *Proceedings of the 10th International Conference on Learning Representations*, pp. 1–20, 2022.
- [29] A. Gupta, P. Dollar, and R. Girshick. LVIS: A Dataset for Large Vocabulary Instance Segmentation. In *Proceedings of the 2019 IEEE/CVF International Conference on Computer Vision and Pattern Recognition*, 2019.
- [30] N. Reimers and I. Gurevych. Sentence-BERT: Sentence Embeddings using Siamese BERT-Networks. In *Proceedings of the 2019 Conference on Empirical Methods in Natural Language Processing*, 2019.